Chemistry
A European
Journal

Chemistry Europe
European Chemical Societies Publishing

Accepted Article

Title: A pH-Induced, Reversible Conformational Switch able to control the Photocurrent Efficiency in a Peptide Supramolecular System

Authors: Emanuela Gatto, Sascha Kubitzky, Mariano Venanzi, Barbara Biondi, Raffaella Lettieri, and Marta De Zotti

To be cited as: *Chem. Eur. J.* 10.1002/chem.202004527

Link to VoR: https://doi.org/10.1002/chem.202004527

WILEY-VCH

10.1002/chem.202004527

A pH-Induced Reversible Conformational Switch able to control the Photocurrent Efficiency in a Peptide Supramolecular System

S. Kubitzky,[a] M. Venanzi,[b] B. Biondi,[c] R. Lettieri,[b] M. De Zotti,*[c] E. Gatto,*[b]

[a] *Faculty of Engineering and Natural Sciences, Technische Hochschule Wildau, Wildau, 15745 Germany*

[b] *Department of Chemical Science and Technologies, University of Rome Tor Vergata, 00133 Rome (Italy)*

[c] *Institute of Biomolecular Chemistry, Padova Unit, CNR, Department of Chemistry, University of Padova, 35131 Padova (Italy)*

Abstract

External stimuli are potent tools that Nature uses to control protein function and activity. For instance, during viral entry and exit, pH variations are known to trigger large protein conformational changes. In Nature, also the electron transfer (ET) properties of ET proteins are influenced by pH-induced conformational changes. In this work, a pH-controlled, reversible 3_{10}-helix to α-helix conversion (from acidic to highly basic pH values and *vice versa*) of a peptide supramolecular system built on a gold surface is described. The effect of pH on the ability of the peptide SAM to generate a photocurrent was investigated, with particular focus on the effect of the pH-induced conformational change on photocurrent efficiency. The films were characterized by electrochemical and spectroscopic techniques, and were found to be very stable over time, also in contact with a solution. They were also able to generate current under illumination, with an efficiency that is the highest recorded so far with biomolecular systems.

KEYWORDS: Supramolecular chemistry, electron transfer, conformational transition, peptides, photocurrent generation.

Introduction

External stimuli are potent tools that Nature uses to control protein activity.[1-4] For instance, pH variations are known to trigger large protein conformational changes, which are crucial for viral entry and exit in the cells.[5,6] In Nature, also the electron transfer (ET) properties of ET proteins (such as azurin and cytochrome c_2) can be influenced by a pH-induced conformational change.[7] In general, peptides and proteins sensitive to pH have basic or acidic amino acids such as lysine, histidine or glutamic acid, which guide peptide or protein pH-induced conformational changes.[5b] In the present work, we investigated the intriguing correlation between pH-triggered 3D-structure

10.1002/chem.202004527

modification and ET on a versatile, peptide-based model system.[8] The final aim of the work is to study the effect of the peptide conformation on the photoinduced ET process and to provide a new biomolecular tool able to modulate ET in response to pH. In the literature, several studies have reported peptide conformational switches induced by pH, both in solution[9-13] and on surfaces.[14-18] Peptide conformational transitions often imply unordered structures as the point of departure or arrival.[19] Conversely, peptides consisting of C^{α}-tetrasubstituted α-amino acids,[20] such as the one exploited in the present work, switch between stable and well defined helical conformations. A secondary structure change may be used to control the ET properties of the analyzed systems. However, this is a complex process, since the ET rate is influenced not only by the backbone structure,[21] but also by the length of the peptide sequence[22-25] and the molecular dynamics of the system.[26] Furthermore, it has been shown that the ET rate for helical peptides depends on the direction in which it proceeds, as a result of the influence of the macrodipole orientation of the helix,[27] spin dependent effects along the helical axis,[28] and the type of helix.[17] The effect of the dipole orientation is bigger in the α-helix than in the 3_{10}-helix conformation, because of the alignment of the amino acid dipoles.[21,29]

The effect of pH on the ET properties of peptide self-assembled monolayers (SAMs) was studied by the group of Kimura, both in the ground state by STM measurements[17] and in photoinduced electron transfer experiments.[16] In the first contribution, they demonstrated that a α-helical peptide is a better ET mediator than the same peptide in the 3_{10}-helix conformation.[17] In the second contribution, the effect of pH on photocurrent generation measurements was studied on a peptide SAM on gold surface, containing a pH sensitive dye.[16] They demonstrated that it was possible to switch the photocurrent direction by changing the pH of the solution, because of the effect of the deprotonation of a free carboxylic group of the dye, that in turn influenced the electric dipole along the helical axis. To our knowledge, no other study has reported the effect of the pH on peptide SAM photocurrent generation, and specifically on the effect of a pH-induced conformational change on photocurrent efficiency.

In a previous study, we succeeded in generating 3D supramolecular films on a gold surface able to generate photocurrent with high efficiency, comparable to the one obtained with non-biological systems.[8] The films have been engineered using different 2D layers, linked together by thymine-adenine DNA base pair interaction. This unconventional way of creating a three dimensional organization of molecules on surface may be applied to build artificial photosynthetic systems able to control the position of the redox centers and the direction of the electronic flow. We

10.1002/chem.202004527

obtained two types of photocurrent-generating films, as shown in Figure 1: Film **1** consisted of adenine linked to lipoic acid (Lipo–A) covalently bound to the gold surface, and a zinc-tetraphenylporphyrin chromophore (ZnTPP) linked to a thymine (T–ZnTPP). Film **2** had an additional noncovalently linked layer: a helical undecapeptide analogue of the natural peptide trichogin GA IV,[30] in which four glycines were replaced by as many lysines to impart water solubility and reduce flexibility.[10,31] The presence of Lys residues also confers pH sensitivity to the peptide secondary structure.[10] The peptide termini were functionalized with thymine and adenine, respectively, to enable Lipo–A and T–ZnTPP conjugation.

In this letter, we describe the effect of the pH-induced, fully reversible, conformational change on the photocurrent generation efficiency of this system. The conformational change of this modular system triggers a different self-assembly on the surface and different electronic conduction properties, leading to its possible exploitation as a pH-responsive biomolecular device.

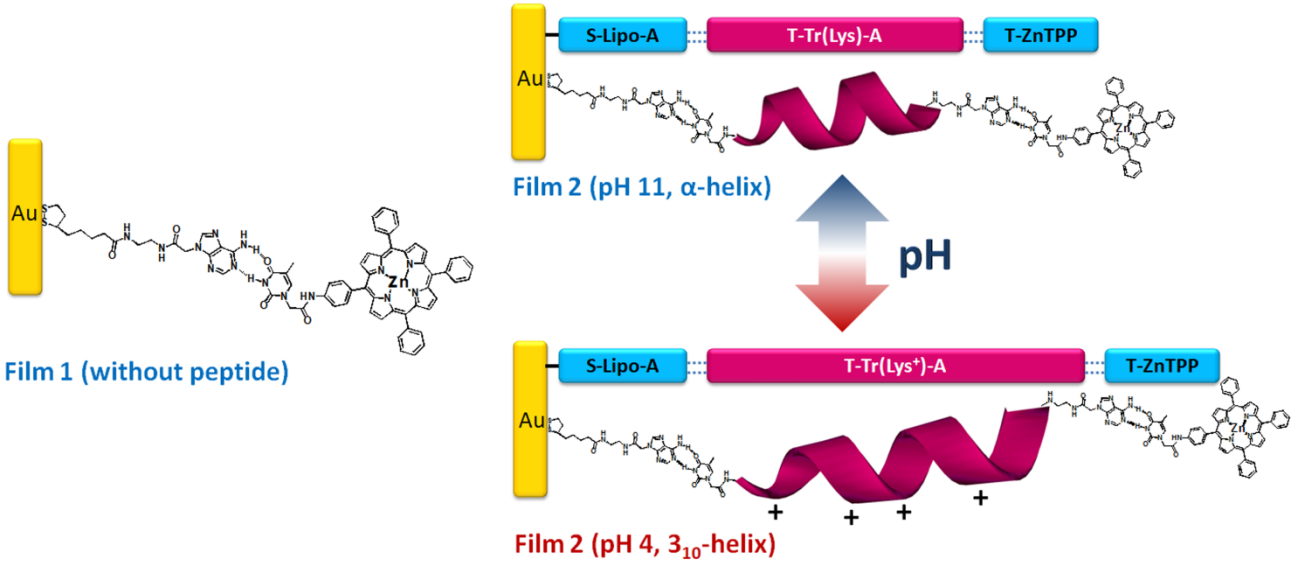

Figure 1. Chemical structures of the building blocks used for the construction of films **1** and **2** and effect of the pH on the film properties.

Results and discussion

Photoconductivity, infrared reflection absorption spectroscopy (IR-RAS), ultraviolet-visible (UV-vis) and fluorescence spectroscopy measurements were carried out for films **1** and **2** after the formation of each layer, and for the final 3D systems in solutions at pH 4 and 11.

The CD spectrum of T-Tr(lys)-A in methanol, reported in SI, exhibits a strong negative band at 204 nm and a weaker negative band at 222 nm, typical of right-handed helical conformations.[32]

10.1002/chem.202004527

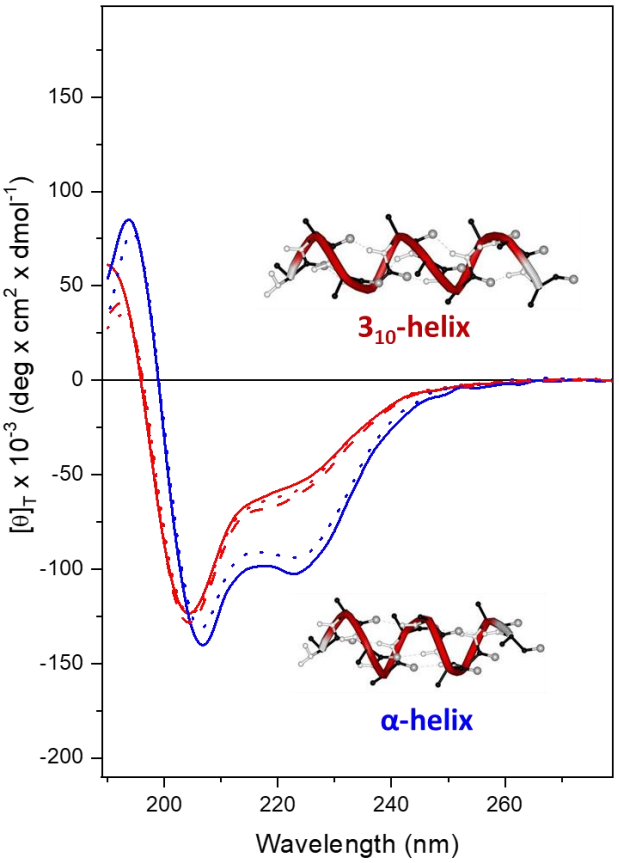

Figure 2. CD spectra of T-Tr(lys)-A in aqueous solution at different pH, c = 1.5•10^{-4} M, l = 0.1 cm. Repeated cycles of helix conversion were performed, in the following order: pH 3 (continuous red line), pH 11 (continuous blue line), pH 2.9 (dotted red line), pH 10.9 (dotted blue line), and pH 3 (dashed red line).

The CD profile of T-Tr(lys)-A in aqueous solution changes substantially from pH 3 to 11 (Figure 2). At pH 3 (*R* value $[\theta]_{222}/[\theta]_{208}$ = 0.4), where all four Lys side chains are protonated,[33-36] the CD profile is clearly indicative of a well developed 3_{10}-helical structure. On the other hand, at pH 11 (*R* value 0.72), where all four Lys side chains are essentially deprotonated, the peptide is folded in a fully developed α-helical structure. Usually, pH-induced peptide conformational transitions are from helix to random coil, due to the electrostatic repulsion after Lys protonation.[37] In the present case, however, three of the eleven residues composing the peptide are C^{α}-tetrasubstituted Aib (α-aminoisobutyric acid) residues, which are known to promote helical conformations, thanks to the steric hindrance of the gem methyl groups on the α carbon.[38,39] As a result, the peptide does not lose its 3D structure upon protonation, but undergoes a reversible conformational transition from α- to 3_{10}-helix. The latter secondary structure has a rise per residue of 2 Å, instead of the 1.5 Å of

10.1002/chem.202004527

the α-helix, making the charges on the Lys residues more distant, thus reducing their electrostatic repulsion. Figure 2 highlights the intriguing phenomenon of pH controlled, reversible 3_{10}- to α-helix conversion (from acidic to highly basic pH values and *vice versa*). This result implies a significant overall contraction (about 5.5 Å) of the peptide backbone following the conformational transition from the longer 3_{10}-helix[40,41] to the shorter α-helix[42] and an associated generation of a biomolecular spring. At this short distance, an elastic super-exchange mechanism, which is characterized by an exponential dependence of k_{ET} on the distance and by a strong dependence on the overpotential,[43] is likely to take place.

The pH induced conformational transition was monitored on surface by IR-RAS measurements (Supporting Information, Figure S2 and S3). A pH-triggered conformational transition from a 3_{10}- to α-helix was already observed for a similar 2D-peptide system on a gold surface.[15] The FTIR-RAS spectrum of the 3D supramolecular structure of film 2 shows the presence of amide I and amide II bands in the range of 1673 cm^{-1} and 1543 cm^{-1}, respectively, confirming the presence of a peptide layer on the surface. Furthermore, the stronger absorbance of amide I compared to amide II and the band positions indicate a helix conformation vertically arranged on the substrate surface.[27d] From pH 4 to pH 11, the amide I band shifts toward higher wavelengths, suggesting, also on gold surface, a conformational transition from 3_{10}- to α-helix (Table 1).[44]

Table 1. IR-RAS data of film **2** in water vapor, previously stabilized in solutions at pH 4 and pH 11.

Sys II	Amide I	Amide II	I_I/I_{II}	Tilt Angle
pH 4	1675	1542	1.8	50°
pH 11	1682	1535	1.1	62°

Calculations based on the amide I/amide II absorbance ratios led to the following tilt angle of the helix axis normal to the surface: 50° at pH 4 and 62° at pH 11. This value is generally obtained for quite good self-assembled peptide monolayers, indicating that the T-Tr(Lys)-A peptide forms a homogeneous film on the Lipo-A layer, despite the low peptide concentration used in the incubation solution to avoid multi-layer formation.[31,45]

10.1002/chem.202004527

The presence of all the three layers was evaluated quantitatively in a previous work.[8] We performed also control experiments by recording UV-Visible spectra before and after the measurements in basic or acidic solutions, to check the film stability in those experimental conditions.

We have already demonstrated that in triethanolamine (TEOA) solution, these films were able to generate current under illumination, with a higher value for film **2** (175 nA/cm^2 at 430 nm) than for film **1** (109 nA/cm^2 at 430 nm), despite the lower ZnTPP content.[8] We thus investigated the effect of the pH on photocurrent generation. We found that upon illumination in the visible region, in Na_2SO_4 solution, high cathodic currents were generated. The electron acceptor in the present system was supposed to be O_2 in solution, since oxygen removal produced a large decrease in the photocurrent signal (Supporting Information, Figure S4). At the same time, however, it has already been reported that H_3O^+ ions may act as electron acceptors in photocurrent generation measurements, considering their high activity from the electrochemical point of view, with a concentration dependent potential.[46] Confirming this hypothesis, a decrease in the solution pH caused a large increase in the photocurrent intensity (Figure 3), because of the higher concentration of H_3O^+ electron acceptors in solution, which increases the ET kinetic. In detail, the photocurrent intensity values at 430 nm were (660$\pm$150) nA/cm^2 for film **2** and (320$\pm$80) nA/cm^2 for film **1** at pH 4, while at pH 11 they became, respectively, (80$\pm$20) and (25$\pm$10) nA/cm^2 (Figure 3). These values are higher than those reported for ZnTPP systems on both indium tin oxide (ITO)[47] and gold[48] surfaces and, at pH 4, represent a quantum efficiency upon excitation at 430 nm[49] of 3.3% for film **2** and 0.7% for film **1**. When a negative potential was applied, the efficiency further increased, reaching the value of 5.1% for film **2** and 1.4% for film **1** at an applied potential of -0.3 V**.** These values are higher than those obtained with other porphyrin-peptide systems covalently linked to a gold surface[50] and, to our knowledge, they are the highest photocurrent values reported so far for bio-based systems.

10.1002/chem.202004527

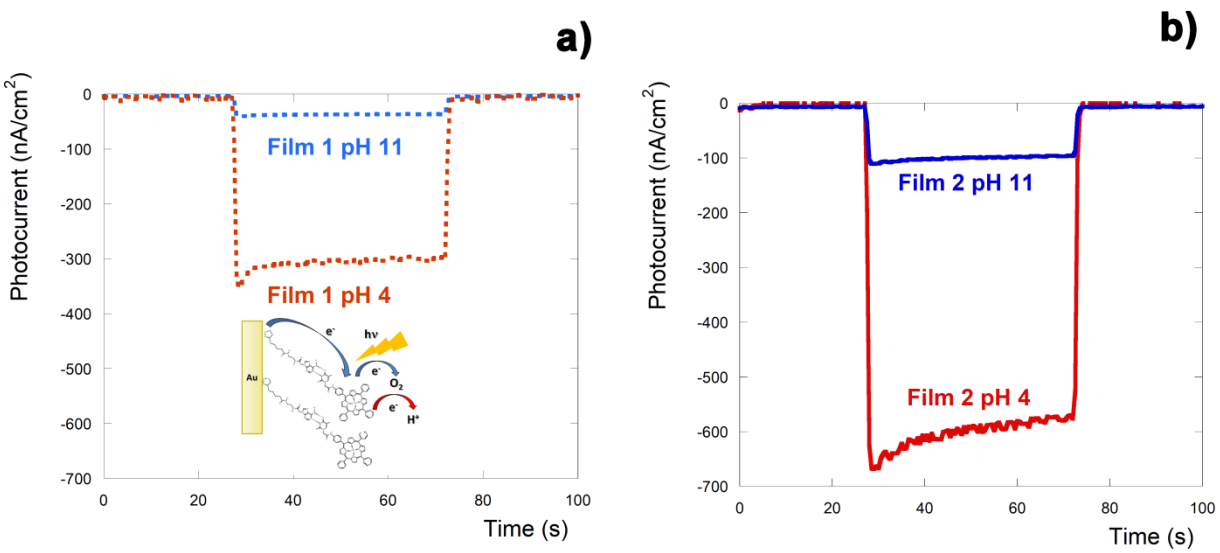

Figure 3. Photocurrent signal obtained by exciting: a) film **1** at λ_{ex} = 430 nm at pH 4 and pH 11 (inset: scheme of the electron flow); b) film **2** at λ_{ex} = 430 nm at pH 4 and pH 11. Applied potential 0 V vs. Ag/AgCl reference electrode.

These results confirm that the system under examination could be the active unit of highly efficient photocurrent generation devices and demonstrate that an increase in the solution pH decreases the photocurrent intensity of both films (because of the ET kinetics reduction caused by the decrease in H_3O^+ acceptor concentration). However, when comparing the photocurrent enhancement of film **2** with that of film **1** at the two pH values, we discovered that the photocurrent improvement was higher at pH 11 (220%), than at pH 4 (106%) (Figure 4). The photocurrent intensity of film **1** is influenced only by the ET kinetic dependence on the concentration of H_3O^+ and O_2 at the two pH values and, for this reason, it is taken as a reference. The higher efficiency of film **2** compared to that of film **1** in generating photocurrent at pH 11 suggests that at this pH value, despite the lower H_3O^+ acceptor concentration and the overall lower value of the photocurrent efficiency, there is some effect which makes film **2** much more efficient than film **1** in generating photocurrent.

10.1002/chem.202004527

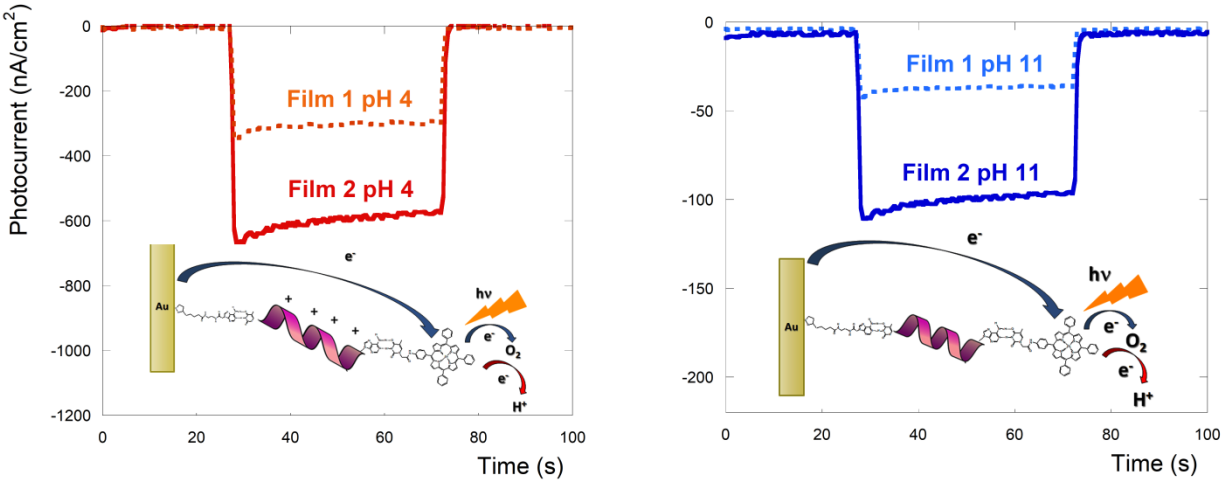

Figure 4. Photocurrent improvement of film **2** compared to film **1** at different pH values, obtained by exciting both films at λ_{ex} = 430 nm, 0 V applied potential vs. Ag/AgCl reference electrode (inset: scheme of the electron flow showing the different peptide conformations at the two pH values).

The reasons for the higher increase of photocurrent value obtained with film **2** compared to film **1** at pH 11 might be multi-fold. First, the trichogin analogue containing lysines [Tr(lys)] undergoes a reversible 3_{10}-helix to α-helix conformational transition (from pH 4 to pH 11) in solution caused by the electrostatic repulsion between the positively charged ε-amino groups of the Lys residues at pH 4. This conformational transition influences the ET rate in two different ways: first, the α-helix is shorter than the 3_{10}-helix. Since the ET rate decreases with the peptide length, the α-helix should be more efficient. Furthermore, it has been demonstrated that the α-helix is more efficient than the 3_{10}-helix in ET processes, because of the alignment of hydrogen bonds in this conformation, compared to the distorted ones found in the 3_{10}-helix.[21]

Second and in contrast to that, the presence of positively charged groups may influence the electronic transport across the peptide. Specifically, Cahen and co-workers demonstrated experimentally that the electronic transport through protonated peptides can lead to an increase in conduction compared to negatively or uncharged peptides, because of the decrease of the energy of both occupied and unoccupied electronic levels.[51] The same conclusion was reported by a theoretical investigation by Tarakeshwar et al.[52] In our system, by decreasing the pH the photocurrent value increases, confirming that protonation improves the photocurrent value; on the other hand, the highest photocurrent difference between film **1** and **2** is obtained at pH 11.

10.1002/chem.202004527

Since the described effects are in contrast, our results demonstrate that the effect of the conformational transition (better ET properties of α-helix compared to 3_{10}-helix) is predominant on that of the charged residues.

To rationalize the better efficiency of film **2** compared to film **1**, we performed absorption and steady state fluorescence experiments on films deposited on a gold (5 nm)-coated glass slide.

The absorption spectra of film **1** and film **2** on Au/glass substrates in air in transmission mode not only confirmed the presence of the T-ZnTPP molecule, but also provided the amount of porphyrin molecules from the measured absorbance value.[8] This value was $(7.0\pm0.5)\cdot10^{-11}$ mol/cm^2 for film **1** and $(3.5\pm0.8)\cdot10^{-11}$ mol/cm^2 for film **2** (with the peptide). Interestingly, the Soret band on the gold surface is broadened and red-shifted by 14 nm for film **2** and 18 nm for film **1**, with respect to the corresponding spectra in methanol (Figure 5). The porphyrin Q-bands were also observed. In general, a red shift is observed in J-aggregates of porphyrins (that is side-by-side porphyrin π-aggregates). However, the red shift observed on gold surface is quite small compared to the one reported in solution,[31,51] indicating a moderate interaction among the porphyrins. In any case, film **2** showed a lower batochromic shift than film **1**, suggesting a higher aggregation in the latter film, confirmed by the higher T-ZnTPP surface density.

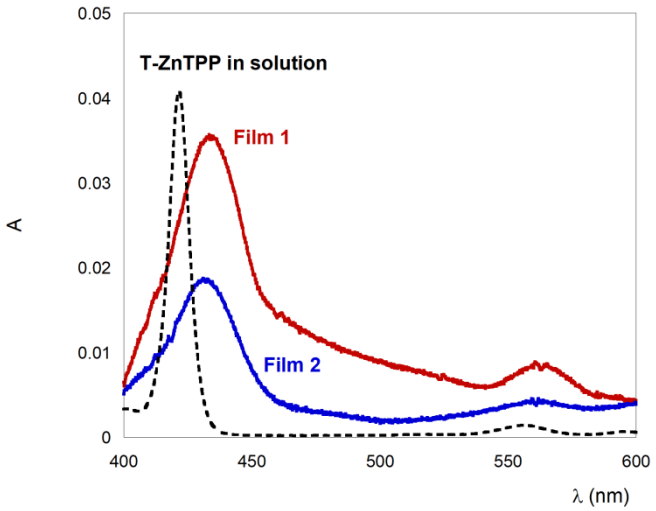

Figure 5. UV-visible spectra of film **1** and **2** on Au/glass surfaces in transmission mode and of T-ZnTPP in methanol solution.

Steady state fluorescence spectra of film **1** and **2** on Au/glass substrates in Na_2SO_4 solution at pH 4 and 11 are shown in Figure 6. Both films exhibit the typical emission band of the ZnTPP fluorophore, with two maxima at 612 and 654 nm, which confirms the T-ZnTPP inclusion into the films. The fluorescence spectra on Au/glass surface are broader compared to those obtained in

10.1002/chem.202004527

solution, and slightly red-shifted, suggesting aggregation among the porphyrins in both films. Interestingly, the fluorescence of film **2** is higher than that of film **1**. It is well known that the porphyrin-excited singlet state is quenched by the gold electrode via energy transfer. This process is distance-dependent and should be more efficient with film **1**, in which the ZnTPP is closer to the gold surface, giving rise to a lower fluorescence intensity. The porphyrin-excited singlet state in solution is quenched also by the O_2 and H_3O^+ dissolved in water and by porphyrin aggregation, which enhances the rate of the nonradiative pathway in the excited state. The lower fluorescence intensity of film **1** (Figure 6) could be caused by the presence of J- aggregates in this film, which enhances the rate of the nonradiative pathway in the excited state. This conclusion is confirmed by the higher bathochromic shift and lower mean molecular area occupied by the T-ZnTPP layer in this film (240 $Å^2$ vs. 476 $Å^2$ for film **2**). Non-fluorescent aggregates in general gives rise to a less efficient photocurrent value,[54] and fluorescence microscopy experiments confirmed this hypothesis, showing wide areas of dark regions in film **1** (Supporting Information, Figures S5 and S6).

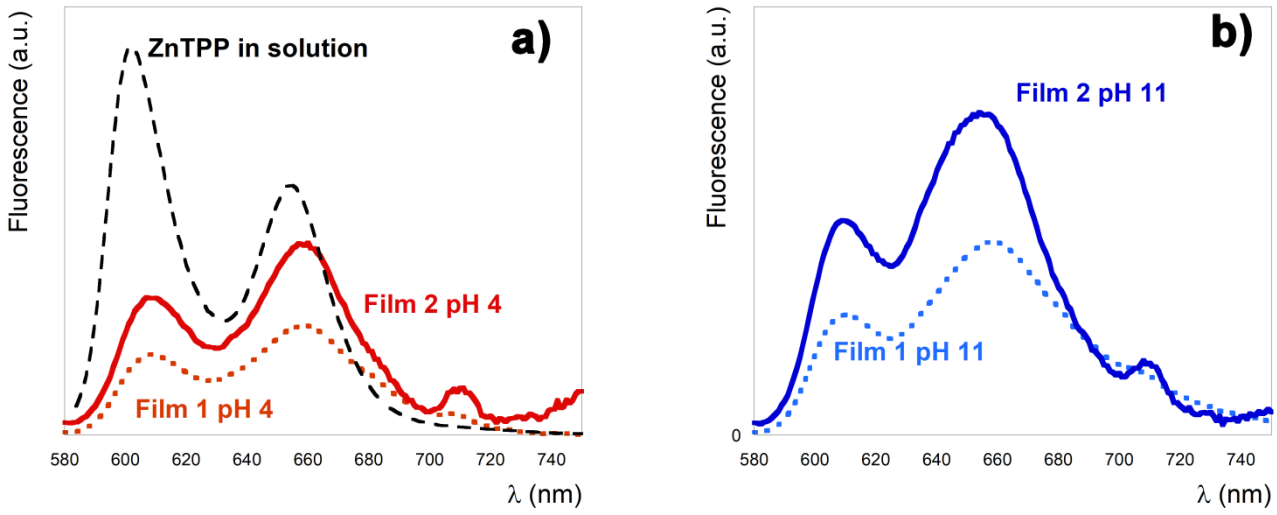

Figure 6. Fluorescence spectra of film **1** and film **2** on Au/glass substrate immersed in an aqueous Na_2SO_4 solution at pH 4 (a) and pH 11 (b) and of T-ZnTPP in methanol solution (a); λ_{ex} = 422 nm in solution and 433 nm on surface. The spectra are normalized for the absorption value at the excitation wavelength.

Figures 6 shows that by increasing the pH, also the fluorescence intensity increases. This is caused by the lower number of H_3O^+ electron acceptors in solution, which reduces the electron transfer quenching kinetics. This can be seen also in film **1**, where no pH effect on the components is expected. However, the steady-state fluorescence enhancement of film **2** relative to film **1** is lower at pH 11 (66%) compared to that observed at pH 4 (75%), as shown in Figure 6. This confirms that

at pH 11, film **2** is much more efficient than film **1** in generating photocurrent. Since the only difference between the two systems is the presence of the peptide, this result suggests that the conformational change induced by the pH makes the α-helix more efficient that the 3_{10}-helix in generating the photocurrent.

Conclusions

The results reported in the present work indicate that pH affects the photocurrent generation process in an effective and simple way, providing a means by which to engineer complex modular supramolecular SAMs able to convert incident light to electronic current, which may find application in photodynamic therapy. This mechanism can be even more effective in an acidic environment, which is in general the chemical condition of tissues in many pathologies, and provide further insight on the influence of the peptide secondary structure on the photocurrent generation efficiency.

Experimental Section

Materials. Spectrograde solvents (Carlo Erba) were exclusively used. Water was distilled and passed through a Milli-Q purification system. Other chemicals, triethanolamine (TEOA) (Fluka), potassium chloride (Carlo Erba), sodium sulphate (Carlo Erba), potassium ferricyanide (Aldrich) and potassium hydroxide (Aldrich) were all of reagent grade quality and used without further purification.

Gold Substrates. Gold foil electrodes of 0.05 mm thickness were bought from Sigma-Aldrich and used for electrochemical measurements. Transparent glass coated with a 5-nm thick Au layer were Nanocs products and used for steady state, time resolved and microscopy fluorescence measurements.

Preparation of Self-assembled Peptide Thin Films. Gold electrodes were etched for 15 min in a freshly prepared piranha solution (2:1 sulphuric acid/H_2O_2, *v/v*), rinsed with bidistilled water and ethanol before immersion in the peptide solution for the SAM deposition. SAM-coated electrodes were prepared by dipping two cleaned gold electrode into an 1 mM methanol solution of Lipo-adenine in a N_2 atmosphere. After 24 h, the electrodes were repeatedly (five times) rinsed with methanol to remove physically adsorbed molecules from the SAM, and immersed into: a 10 μM peptide solution for film **2** and a 0.1 mM T-ZnTPP solution for film **1**. After 24 h, the electrode containing film **1** (Au/Lipo-A•••T-ZnTPP) was dried for 3 min under a gentle argon flow and was ready to be used, while the second electrode was let into the T-Tr(Lys)-A solution for 48 h. After this time, it was dipped into a 0.1 mM solution of T-ZnTPP in a N_2 atmosphere, in order to obtain the three layer system. Subsequent to 24 h, the electrode containing film **2** (Au/Lipo-A•••T-Tr(Lys)-A •••T-ZnTPP) was dried for 3 min under a gentle argon flow and was ready to be used.

10.1002/chem.202004527

Methods. *Electrochemistry.* Cyclic voltammograms (CVs) were obtained by using a PG 310 potentiostat (Heka Elektronik). CV experiments were carried out at room temperature, adopting a standard three-electrode configuration with a SAM-coated gold electrode as the working electrode, a platinum wire as the auxiliary electrode, and Ag/AgCl as the reference electrode. Experiments to determine the surface area of Au gold foil electrodes were carried out with a 0.5 mM $K_3Fe(CN)_6$ solution in 1 M KCl at a sweep rate of 50 $mV \cdot s^{-1}$. Photocurrent measurements were carried out at room temperature using the three-electrode set-up described above, by using Na_2SO_4 (0.1 M) as supporting electrolyte. In this experiment, the SAM-modified electrode was irradiated with a Xe lamp (150 W) equipped with a monochromator and the generated photocurrent was detected by the voltammetric analyzer described above. The incident photon-to-current efficiency (IPCE) has been determined by using the following equation:[6]

$$IPCE\,(\%) = \frac{100 \cdot i\left(A/cm^2\right) \cdot 1240}{I\left(W/cm^2\right) \cdot \lambda(nm)}$$

where *i* is the measured photocurrent, *I* is the incident light power density, and λ is the incident wavelength (340 nm). The intensity of the incident light was evaluated with a Vector H410 Power Meter (Scientech, USA) and the yields of photocurrent generation were obtained using the following equation:[7]

$$\phi = \frac{\frac{i}{e}}{\frac{W \cdot \lambda}{h \cdot c}(1 - 10^{-A})}$$

where I=W•λ /h•c, is the number of photons per unit area and unit time, i is the photocurrent density, e is the elementary charge, λ the wavelength of light irradiation, A the absorbance of the adsorbed dyes at λ, W the light power irradiated at λ, c the velocity of light, and h the Planck constant.

The solution pH was modified by adding HCl 3M and NaOH 3M solutions and measuring the value with a pH meter.

UV-Visible absorption measurements. UV-Visible absorption measurements were carried out on a Varian Cary 100 Scan spectrophotometer (Middelburg, The Netherlands) at room temperature. The nude substrate has been used as baseline.

Steady-state Fluorescence. Steady-state fluorescence experiments were carried out on a Fluoromax-4 spectrofluorimeter (Jobin-Yvon) operating in the single-photon counting mode. For the fluorescence measurements, the peptide SAMs were immobilized on a transparent glass coated with a 5-nm thick Au layer. The glass was mounted on a solid sample holder and the signal detected at 45°. The tilt angle between the light source and the detector has been optimized in order to maximize the signal/noise ratio. The measurements in solution have been performed by inserting the surface into a quartz cuvette, filled with the Na_2SO_4 (0.1 M) solution, taking care of maintaining the tilt angle of 45° between the light source and the detector, and operating in transmission mode. The pH was changed by adding HCl and NaOH solutions.

10.1002/chem.202004527

Circular Dichroism. CD spectra were recorded using a J600 spectropolarimeter from Jasco (Tokyo, Japan). The temperature was controlled at 25 ± 0.1 °C with a thermostatted cuvette holder. The reported CD signals were normalized with respect to peptide molar concentrations. *CD*. The pH switch tests were carried out starting from 3 mL of a stock solution at 10^{-4} M concentration in water. Before each analysis, the pH was measured using a pH meter. For each test exactly 300 µL were inserted into the CD cuvette (optical path 1mm) and, at the end, all the contents of the cuvette were carefully extracted and put back into the mother solution where a few microliters of the aqueous solutions of HCl 3M or NaOH 3M were added. This method allows to test the reversibility of the structural interconversion mediated by the pH: without working in the same solution one could only say that the peptide assumes that type of conformation at a certain pH and not that the peptide actually has the ability to change reversibly conformation.

The curves have been normalized for the concentration, thus removing the error caused by the loss of solution due to the transfers and the addition of the acid and base solutions.

Fourier transform infrared reflection-absorption spectroscopy (FTIR-RAS). FTIR-RAS experiments were performed by using a Thermo-Scientific (mod. Is50) instrument (Thermo Scientific Inc., Madison, WI, USA), with a VeemaxTM III Variable Angle reflectance Accessory (Pike Technologies, Madison, WI, USA) and a mercury-cadmium-telluride (MCT) detector. Moreover, a polarized incident beam at an incidence angle of 80° with respect to the sample surfaces was used. A total of 516 scans, with a resolution of 2 cm^{-1}, were collected for each sample. The pH experiments have been performed by immersing the films on gold surface into a basic or acid solution for five minutes, then they have been dried with an argon flow and finally they have been measured at controlled water vapor.

ASSOCIATED CONTENT

Circular dichroism spectrum of T-Tr(lys)-A in methanol, IR-RAS spectra of the two films, photocurrent signal after oxygen removal, fluorescence spectra of the two films on the surface by changing the solution pH, fluorescence microscopy images of the two films on surface, synthesis of all the building blocks and their HPLC and NMR characterization, TEM images of the fibers formed by T-Tr(lys)-A in acetonitrile. This material is available free of charge.

AUTHOR INFORMATION

Corresponding authors: Emanuela Gatto: emanuela.gatto@uniroma2.it; Marta De Zotti: marta.dezotti@unipd.it

NOTES

The authors declare that they have no competing financial interests.

ACKNOWLEDGEMENTS

This work was supported by MIUR (Rome, Italy) (Futuro in Ricerca 2013, grant no. RBFR13RQXM and PRIN project 20173LBZM2). MDZ is grateful to the University of Padova (Italy) for funding (project P-DiSC#04BIRD2019-UNIPD). We thank dr. Claudia Mazzuca for assistance in RAS measurements.

REFERENCES

[1] C. Valéry, S. Deville-Foillard, C. Lefebvre, N. Taberner, P. Legrand, F. Meneau, C. Cristelle Meriadec, C. Camille Delvaux, T. Bizien, E. Kasotakis, C. Lopez-Iglesias, A. Gall, S. Bressanelli, M. E. Le Du, M. Paternostre, F. Artzner. *Nature Commun.* **2015**, *6*, 7771.

[2] J. Wang, L. Zhang, J. Yang, H. Yan, X. Li, C. Wang, D. Wang, Y. Sun, H. Xu. *Langmuir* **2019,** *35*, 5617-5625.

[3] E. Gatto, M. E. Palleschi, B. Zangrilli, M. De Zotti, B. Di Napoli, A. Palleschi, C. Mazzuca, F. Formaggio, C. Toniolo, M. Venanzi. *Peptide Science* **2018**, *110*, e24081.

[4] J. Srivastava, D. L. Barber, M. P. Jacobson. P*hysiology* **2007**, *22*, 30–39.

[5] (a) T. Stegmann, F. P**. B**ooy, J. Wilschut, *J. Biol. Chem.* **1987,** *262,* 17744-17749; (b) A. Helenius, *Nature Cell Biol.* **2013,** *15,* 125.

[6] V. C. Chu, L. J. McElroy, V. Chu, B. E. Bauman, G. R. Whittaker, *J. Virol.* **2006**, *80*, 3180–3188.

[7] N. K. Rogers, G. R. Moore, *FEBS Lett.* **1988**, *228*, 69-73.

[8] E. Gatto, S. Kubitzky, M. Schriever, S. Cesaroni, C. Mazzuca, M. Venanzi, M. De Zotti. *Angew. Chem. Int. Ed.* **2019**, *58*, 7308-7312.

[9] (a) A. Bañares-Hidalgo, J. Pérez-Gil, P. Estrada. *Biochim. Biophys. Acta Biomemb*. **2014**, *1838*, 1738-1751; (b) C. S. H. Jesus, P. F. Cruz, L. G. Arnaut, R. M. M. Brito, C. Serpa, *J. Phys. Chem. B* **2018**, *122*, 3790-3800.

[10] M. De Zotti, B. Biondi, C. Peggion, F. Formaggio, Y. Park, K. S. Hahm, C. Toniolo, *Org.Biomol. Chem.* **2012**, *10*, 1285-1299.

[11] R. Cerpa, F. E. Cohen, I. D. Kuntzù, *Fold. Des.* **1989**, *1*, 91-101.

[12] (a) M. Barteri, B. Pispisa, *Biopolymers* **1973,** *12*, 2309-2327; (b) Y. P. Myer, *Macromol.* **1969**, *2*, 624-628.

[13] J. H. Ha, S. N. Loh, *Chemistry*, **2012**, 18, 7984–7999.

[14] T. Doneux, L. Bouffier, L. V. Mello, D. J. Rigden, I. Kejnovska, D. G. Fernig, S. J. Higgins, R. J. Nichols. *J. Phys. Chem. C* **2009**, *113*, 6792–6799.

[15] G. M. L. Messina, B. Di Napoli, M. De Zotti, C. Mazzuca, F. Formaggio, A. Palleschi, G. Marletta. *Langmuir* **2019**, *35*, 4813-4824.

[16] S. Yasutomi, T. Morita, S. Kimura, *J. Am. Chem. Soc.* **2005**, *127*, 14564-14565.

[17] K. Kitagawa, K.; T. Morita, T.; S. Kimura, S. *Angew. Chem. Int. Ed.* **2005**, *44*, 6330-6333.

[18] L. Scullion, T. Doneux, L. Bouffier, D. G. Fernig, S. J. Higgins, D. Bethell, R. J. Nichols. *J. Phys. Chem. C* **2011**, *115*, 8361–8368.

[19] (a) M. Mutter, R. Gassmann, U. Buttkus, K. H. Altmann, *Angew. Chem. Int. Ed.* **1991**, *30*, 1514-1516; (b) A. Fissi, O. Pieroni, E. Balestrieri, C. Amato, Macromolecules **1996**, *29*, 4680-4685; (c) A. Aemissegger, D. Hilvert, *Nat. Protocols* **2007**, *2*, 161-167; (d) M. Blanco-Lomas, S. Samanta, P. J. Campos, G. A. Wooley, D. Sampedro, *J. Am. Chem. Soc.* **2012**, *134*, 6960-6963.

[20] C. Toniolo, M. Crisma, F. Formaggio, C. Peggion, *Biopolymers- Pept. Sci.* **2001**, *60*, 396-419.

[21] Y. N. Shin, M. D. Newton, S. S. Isied. *J. Am. Chem. Soc.* **2003**, *125*, 3722-3732.

[22] R. Abdel Malak, Z. Gao, J. F. Wishart, S. S. Isied. *J. Am. Chem. Soc.* **2004**, *126*, 13888-13889.

[23] S. S. Isied, M. Y. Ogawa, J. F. Wishart. *Chem. Rev*. **1992**, 92, 381-394.

[24] T. Morita, T.; S. Kimura, S. *J. Am. Chem. Soc.* **2003**, *125*, 8732-8733.

[25] M. Sisido, R. Tanaka, Y. Inai, Y. Imanishi. *J. Am. Chem. Soc*. **1989,** 111, 6790-6796.

[26] (a) G. A. Orlowski, S. ChowDhury, H. B. Kraatz. *Langmuir* **2007**, *23*, 12765-12770; (b) K. Takeda, T. Morita, S. Kimura. *J. Phys. Chem. B* **2008**, *112*, 12840-12850.

[27] (a) M. Lauz, S. Eckhardt, K. M. Fromm, B. Giese, *Phys. Chem. Chem. Phys.* **2012**, *14*, 13785-13788; (b) S. Yasutomi, T. Morita, Y. Imanishi, S. Kimura, *Science* **2004**, *304*, 1944-1947; (c) S. Sek, A. Tolak, A. Misicka, B. Palys, R. Bilewicz, *J. Phys. Chem. B* **2005**, *109*, 18433–18438; (d) J. Watanabe, T. Morita, S. Kimura, *J. Phys. Chem. B* **2005**, *109*, 14416–14425; (e) E. Galoppini, Fox, M. A. *J. Am. Chem. Soc*. **1996,** *118*, 2299-2300.

[28] (a) A. C. Aragonès, E. Medina, M. Ferrer-Huerta, N. Gimeno, M. Teixidó, J. L. Palma, N. Tao, J. M. Ugalde, E. Giralt, I. Díez-Pérez, V. Mujica, *Small* **2017**, 13, 1602519; (b) M. Kettner, B. Göhler, H. Zacharias, D. Mishra, V. Kiran, R. Naaman, C. Fontanesi, D. H. Waldeck, S. Sek, J. Pawlowski, J. Juhaniewicz, *J. Phys. Chem. C* **2015**, *119*, 14542-14547; (c) F. Tassinari, D. R.

Jayarathna, N. Kantor-Uriel, K. L. Davis, V. Varade, C. Achim, R. Naaman, *Adv. Mater.* **2018**, 1706423.

[29] (a) S. Umehara, N. Pourmand, C. D. Webb, R. W. Davis, K. Yasuda, M. Karhanek, *Nano Letters* **2006**, *6*, 2486-2492; (b) E. Gatto, A. Porchetta, L. Stella, I. Guryanov, F. Formaggio, C. Toniolo, B. Kaptein, Q. B. Broxterman, M. Venanzi, *Chem. Biodivers.* **2008**, *5*, 1263-1278; (c) E. Gatto, L. Stella, F. Formaggio, C. Toniolo, L. Lorenzelli, M. Venanzi, M. *J. Pept. Sci.* **2008**, *14*, 184-191.

[30] C. Peggion, F. Formaggio, M. Crisma, R. F. Epand, R. M. Epand, C. Toniolo, *J. Pept. Sci.* **2003**, *9*, 679-689.

[31] G. Marafon, I. Menegazzo, M. De Zotti, M. Crisma, C. Toniolo, A. Moretto. *Soft Matter* **2017**, *13*, 4231-4240.

[32] C. Toniolo, A. Polese, F. Formaggio, M. Crisma, J. Kamphuis. *J. Am. Chem. Soc.* **1996***, 113*, 2744.

[33] C. Toniolo, M. Crisma, F. Formaggio, C. Peggion, V. Monaco, C. Foulard, S. Rebuffat, B. Bodo. *J. Am. Chem. Soc.* **1996**, *118*, 4952.

[34] P. M. Hardy, in Chemistry and Biochemistry of the Amino Acids; ed. G.C. Barrett, Chapman and Hall, London, **1985**, pp. 6–24.

[35] I. André, S. Linse, F. A. A. Mulder, J. Am. Chem. Soc. **2007**,129, 15805–15813.

[36] K. Wüthrich. NMR of Proteins and Nucleic Acids, Wiley, New York, 1986.

[37] B. Pispisa, M. Venanzi, A. Palleschi, J. Chem. Soc., Faraday Trans. **1994**, 90, 1857-1864.

[38] (a) E. Gatto, M. Venanzi, *Polym. J. 2013, 45, 468-480; (b)* M. Venanzi, E. Gatto, G. Bocchinfuso, A. Palleschi, L. Stella, C. Baldini, F. Formaggio, C. Toniolo. *J. Phys. Chem. B **2006**, 110, 22834-22841;* (c) M. Venanzi, E. Gatto, G. Bocchinfuso, A. Palleschi, L. Stella, F. Formaggio, C. Toniolo, *ChemBioChem **2006**, 7, 43-45;* (d) M. Venanzi, G. Bocchinfuso, E. Gatto, A. Palleschi, L. Stella, F. Formaggio, C. Toniolo, *ChemBioChem* **2009**, *10,* 91-97.

[39] (a) P. Balaram, *Curr. Opin. Struct. Biol.* **1992**, *2,* 845-851; (b) C. Toniolo, M. Crisma, F. Formaggio, C. Peggion, *Biopolymers (Pept. Sci.)* **2001**, *60,* 396-419.

[40] C. Toniolo, E. Benedetti. Trends Biochem. Sci. **1991**, 16, 350–353.

[41] Y. T. Long, E. A. Irhayem, H. B. Kraaz, H. B. Chem Eur. J. **2005**, 11, 5186-5194.

[42] Y. Miura, S. Kimura, S. Kobayashi, M. Iwamoto, Y. Imanishi, U. Umemura. Chem. Phys. Lett. **1999**, 315, 1-6.

[43] E. Gatto, M. Caruso, M. Venanzi, *The Electrochemistry of Peptide Self-Assembled Monolayers.* In: Aliofkhazraei M., Makhlouf A. (eds) Handbook of Nanoelectrochemistry. Springer, Cham., **2016**.

[44] H. Maekawa, C. Toniolo, Q. B. Broxterman, N. H. Ge. *J. Phys. Chem. B* **2007**, *111,* 3222-3235; (b) R. A. Silva, S. C. Yasui, J. Kubelka, F. Formaggio, M. Crisma, C. Toniolo, T. A. Keiderling. *Biopolymers* **2002**, *65*, 229-243.

[45] G. Marafon, D. Mosconi, D. Mazzier, B. Biondi, M. De Zotti, A. Moretto, *RSC Adv.* **2016**, 6, 73650-73659.

[46] T. Morita, S. Kimura, S. Kobayashi, Y. Imanishi, *J. Am. Chem. Soc.* **2000**, *122*, 2850–2859.

[47] H. Yamada,; H. Imahori,; Y. Nishimura, I. Yamazaki,; S. Fukuzumi, *Advanced Mater.* **2002**, *14*, 892-895; (b) H. Imahori, M. Kimura, K. Hosomizu, T. Sato, T. K. Ahn, S. K. Kim, D. Kim, Y. Nishimura, I. Yamazaki, Y. Araki, O. Ito, S. Fukuzumi, *Chem. Eur. J.* **2004**, *10*, 5111 – 5122.

[48] H. Imahori, H. Norieda, Y. Nishimura, I. Yamazaki, K. Higuci, N. Kato, T. Motohiro, H. Yamada, K. Tamaki, M. Arimura, Y. Sakata, *J. Phys. Chem. B* **2000**, *104*, 1253–1260; (b) H. Imahori, T. Hasobe, H. Yamada, Y. Nishimura, I. Yamazaki, S. Fukuzumi, *Langmuir* **2001**, *17*, 4925-4931.

[49] E. Gatto, A. Porchetta, M. Scarselli, M. De Crescenzi, F. Formaggio, C. Toniolo, M. Venanzi. *Langmuir* **2012**, 28, 2817-2826.

[50] H. Uji, Y. Yatsunami, S. Kimura. J. Phys. Chem. C **2015,** 119, 8054-8061; (b) H. Uji, K. Tanaka, S. Kimura. J. Phys. Chem. C **2016**, 120, 7, 3684-3689*; (c)* A. Vecchi, E. Gatto, B. Floris, V. Conte, M. Venanzi, V. N. Nemykin, P. Galloni, *Chem. Commun*. **2012**, *48*, 5145-5147.

[51] L. Sepunaru, S. R. Abramson, R. Lovrincic, J. Gavrilov, P. Agrawal, J. Levy, L. Kronik, I. Pecht, M. Sheves, D. Cahen. *J. Am. Chem. Soc.* **2015**, *137*, 9617-9626.

[52] P. Tarakeshwar, J. L. Palma, G. P. Holland, P. Fromme, J. L. Yarger, V. Mujica. *Phys. Chem. Lett.* **2014**, *5*, 3555-3559.

[53] J. R. Lakowicz, Principles of Fluorescence Spectroscopy, Plenum Press, New York, **1983**.

[54] E. Gatto, A. Quatela, M. Caruso, R. Tagliaferro, M. De Zotti, F. Formaggio, C. Toniolo, A. Di Carlo, M. Venanzi**,** *ChemPhysChem* **2014**, *15*, 64-68.

10.1002/chem.202004527

TOC

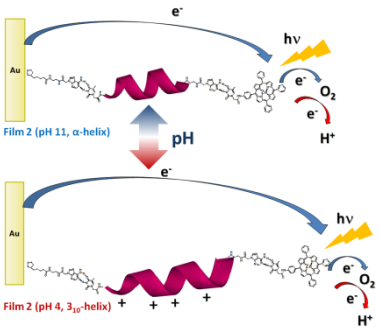

A supramolecular peptide-based bio-inspired systems have been built on gold surface. The effect of pH on the peptide conformation and on the ability of the film to generate photocurrent was investigated. In particular, at low pH the photon to current conversion efficiency obtained, is the highest value recorded so far with biomolecular systems.